Research of a cusped field thruster using different wall materials

IEPC-2015-403／ISTS-2015-b-403

Presented at Joint Conference of 30th International Symposium on Space Technology and Science 34th International Electric Propulsion Conference and 6th Nano-satellite Symposium, Hyogo-Kobe, Japan July 4 – 10, 2015

Guoshun Sun[1], Hui Liu.[2], Daren Yu, Pengbo Chen, Chengyu Ma
Institute of Advanced Power, Harbin Institute of Technology, Harbin, Heilongjiang Province, 150001, CHINA

Abstract: The cusped field thruster is an emerging kind of electric propulsion devices with the advantage of high ionization rate and long life. It was early recognized that the type of material used for the walls of the discharge channel had a significant impact on the characteristics of the plasma. To study the influences wall material has on the performance of cusped field thruster, especially Secondary Electron Emission, this article conducted a systematic experiment on thruster using different wall materials: boron nitride, silicon carbide, alumina. Experimental results showed that to achieve the optimal performance, secondary emission yield of material need match with the operating conditions. And the peak-to-peak values of anode current oscillation showed that the thruster operates relatively steadily using alumina as wall material.

I. Introduction

THE cusped field thruster is an emerging kind of electric propulsion device appeared in recent years. As shown in Fig.1, the discharge channel is surrounded by multistage permanent magnets, and two adjacent ones have the opposite polarity to form the cusped magnetic field. Electrons emitted by cathode to the discharge channel to ionize the working gas injected from the upstream gas distributor. The magnetic field lines away from cusps are mainly parallel with the discharge channel wall, combined with strong magnetic mirror effect at the cusp, the plasma can be confined effectively to enhance ionization and limit the interaction between plasma and discharge channel wall. So the thruster has high ionization rate and long lifetime.[1] The first kind of this thruster is the High Efficiency Multistage Plasma thruster (HEMP) developed by Thales Electron Devices in 1998, and it is scheduled to be operated on the SmallGEO satellite platform.[2] Due to its remarkable characteristics, it also attracts attention of other institutions, such as MIT’s diverging cusped field thruster (DCFT) and Stanford’s cylindrical cusped field thruster (CCFT).[3,4,5]

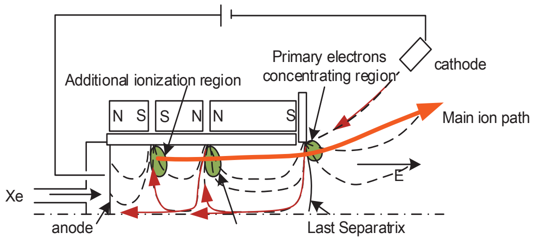

Figure 1. Cusped field thruster operation principle

A 4000h’ endurance testing of HEMP showed that the thrust steadily decreased with running time from the value of 44.5mN to 40.1mN after 2900 integrated hours, along with the progressively increase of the thruster temperature and the decrease of anode current. This decrease is induced by the successively built-up of a conductive graphite layer on the discharge channel due to re-deposition of vacuum chamber material eroded by thruster ion beam impingement. After removing the conductive graphite layer, the data collected after the test restart demonstrated a full recovery of

[1] Postgraduate, Energy Science and Engineering, Harbin Institute of Technology, hit_sgs@163.com.
[2] Lecturer, Institute of Advanced Power, Harbin Institute of Technology, thruster@126.com.

thruster performance. And the experiment in a test facility modified with the Aluminum coating showed a steady performance, demonstrating that wall material has an influence on cusped field thruster.[1] However, the influence of wall material has on cusped field thruster was not studied separately. Most researches of wall materials focused on the Hall thruster.[6, 7, 8] One of the most remarkable works in this area was led by Bugrova with the aim of verifying some predictions of the so-called near-wall conductivity theory developed by Morozov.[9]

It was early recognized that the type of wall material of the discharge channel had a significant impact on the characteristics of the plasma and on the ion acceleration process. The wall material of mainstream electric propulsion devices like Hall thrusters and ion thrusters is boron nitride (BN). The main influence factors of wall materials on thruster performance are Secondary Electron Emission and near-wall Conductivity (caused by the collisions with walls) by the researches on Hall thrusters.[6,9,10] In such a discharge, due to the high electric conductivity perpendicularly to the channel walls (i.e., along the magnetic field lines), the high energy electrons are continuously replaced by low energy secondary electrons, resulting in a limitation of electron temperature and temperature gradients to moderate values. The magnetic field lines away from cusps are mainly parallel with the discharge channel wall, combined with strong magnetic mirror effect at the cusp, the plasma can be confined effectively to limit the interaction between plasma and discharge channel wall.[1] It can be reasonably inferred that the influences of Secondary Electron Emission and near-wall Conductivity are relatively small. To study the mechanism of plasma-wall interaction and the influences Secondary Electron Emission has on thruster performance, there are experimental studies on thrusters with different wall material BN, silicon carbide (SiC), alumina (Al_2O_3) (secondary emission yield increasing in order).

Besides, limited by diagnostic method, Particle-in-cell simulation was used to analyze the effect of secondary emission yield on plasma parameters of a cusped field thruster. Some works concerning the PIC-MCC simulation of cusped field thruster have already been done. R. Schneider's PIC-MCC simulated results demonstrated that the HEMPT-type cusped field thruster allows for good performance due to both minimal energy dissipation and high acceleration efficiency.[11] The interaction between the plasma and the wall is limited only to regions with magnetic field cusps, which results in much smaller ion flux to the thruster channel surface than Hall Thrusters. R. Gildea et al have simulated divergent cusped-field thrusters (DCFT) by using the PIC-MCC method and revealed some physical process of the plasma under the specific cusped magnetic field topology.[12] In addition, Y J Zhao et al have simulated the effect of magnetic field strength on a cusped field thruster.[13]

II. Experimental Setup

A. Experiment Setup

The experiments are conducted in the vacuum tank of plasma propulsion laboratory of Harbin Institute of Technology (HPPL). The tank has a length of 4m and an inner diameter of 1.2m. The ultimate pressure in the tank can reach 1.0×10^{-3}Pa. The purity of any kind of propellants used in experiment is in excess of 99.999%. The thrust is measured with a torsion balance. It transforms the thruster force to an equivalent rotation angle and then an equivalent linear displacement of a third medium. The third medium that we use here is a laser spot which is reflected to shift by a mirror fixed on the balance. The balance needs to be calibrated with standard weights before used. The anode current was monitored by a filtering oscilloscope. The cathode electron exit was fixed at horizontal 50mm and vertical 50mm to thruster channel exit center. The cathode flow rate was fixed at 3sccm and the keeper voltage was kept at 21V. The thruster performance with different anode mass flow rate and discharge voltage was tested. The power supply which offered anode voltage could range from 0V to 500V. The anode mass flow rate of working gas could be varied from 0sccm to 50sccm.

B. Thruster

The experimental prototype of cusped field thruster designed by HIT is used in this experiment, as shown in Fig.2. The thruster weighs 4.5kg with a discharge channel 35mm in diameter and 112mm in radial length, and a relatively deep channel is good for ionization. The most distinctive feature of this thruster is modular design. As shown in Fig.2, the magnetic field of cusped field thruster can be changed conveniently because of modular magnet. And the shell of thruster and radiator are also using modular design to change the location of radiator and length of shell. The magnetic field

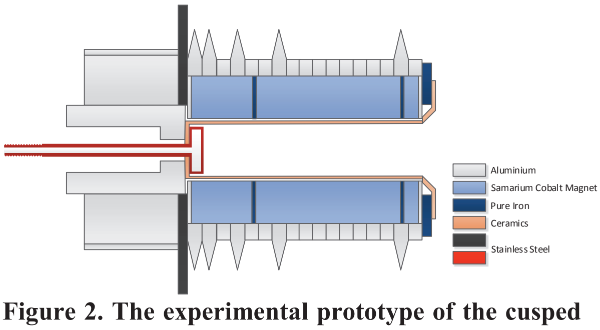

Figure 2. The experimental prototype of the cusped field thruster designed by HIT.

distribution of this thruster is shown in Fig.3. The scheme has three stages formed by magnets and magnetic rings, and magnet near exit is longer. An additional small ring magnet with opposite polarity and a pure iron ring are placed at the exit plane. The additional ring magnet is arranged with a polarity repelling the most downstream magnetic field lines to form a flat downstream separatrix. And the purpose of the pure iron is to weaken the magnetic field in plume region. So thruster operates steadily, and plume is controlled effectively.[14]

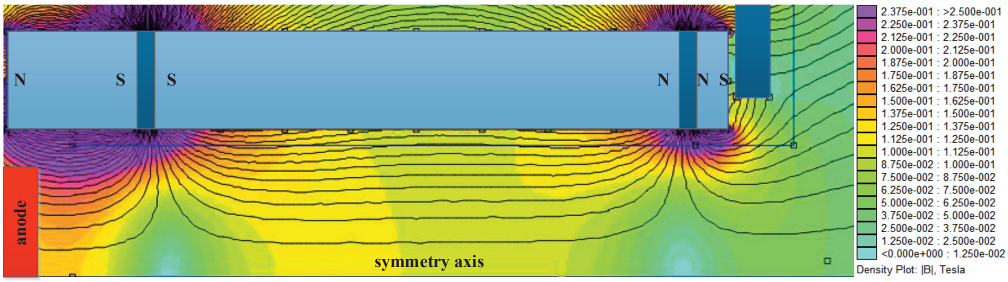

Figure 3. Magnetic field distribution of the cusped field thruster.

III. Experimental Result and Discussion

Performance measurements were collected in two sets of experiments. In the first set of experiments, the variable-voltage performance of thruster with different wall materials was studied. This series was conducted over the range 100V - 500V in 50V increments at constant anode mass flow rate of 10sccm and 20sccm. This flow rate was chosen so that the discharge power would be suitable at high anode voltage, thus minimizing the risk of thermally induced failure of the thruster. Future testing is planned at higher flow rate and correspondingly higher efficiency. And in the second set of experiments, the variable-flow performance of thruster with different wall materials was studied. This series was conducted over the range 10sccm - 40sccm in 5sccm increments at a constant anode voltage of 300V.

A. Variable-Voltage Performance

It was obvious that performance characteristics (anode current, thrust, efficiency) of cusped field thruster using different wall materials as discharge channel were different. What should be explained was using SiC as channel wall. Discharge current increased quickly at 500V, 10sccm or above 200V, 20sccm (corresponds to the power above 500W). Seeing from Fig.4, thrust increased steadily, showing that the sudden increase of discharge current was not related to ionization. And it can be inferred that the increase of electron current (probably caused by thermally induced failure of the magnetic field) is responsible for the performance reduction. Especially at 20sccm, above 350V, with the phenomenon of the channel at the cusp reddening and obvious oscillation, experiment stopped to avoid failure of thruster. After test restarting, thruster showed similar performance evolution as during the first test. Then wall materials BN and Al_2O_3 were mainly analyzed.

Figure 4 depicts typical performance characteristics of the cusped field thruster as functions of discharge voltage for all tested materials. As shown in Fig.4, at constant anode flow rate of 10sccm and 20sccm, the differences of anode current and thrust were relatively small for three materials at a low anode voltage. At a high anode voltage, the discharge current and thrust of BN were greater than Al_2O_3, and the difference of discharge current reached to 0.12A at 500V. Thrust of BN and Al_2O_3 reached to the maximum values of 34.05mN, 33.16mN, respectively. But the efficiency of Al_2O_3 was slightly greater than BN, and the efficiency advantage of Al_2O_3 declined with the increase of anode flow rate. At the same time, the peak-to-peak values of anode current oscillation (monitored by a filtering oscilloscope) showed that the thruster operates relatively steadily using Al_2O_3 as channel wall.

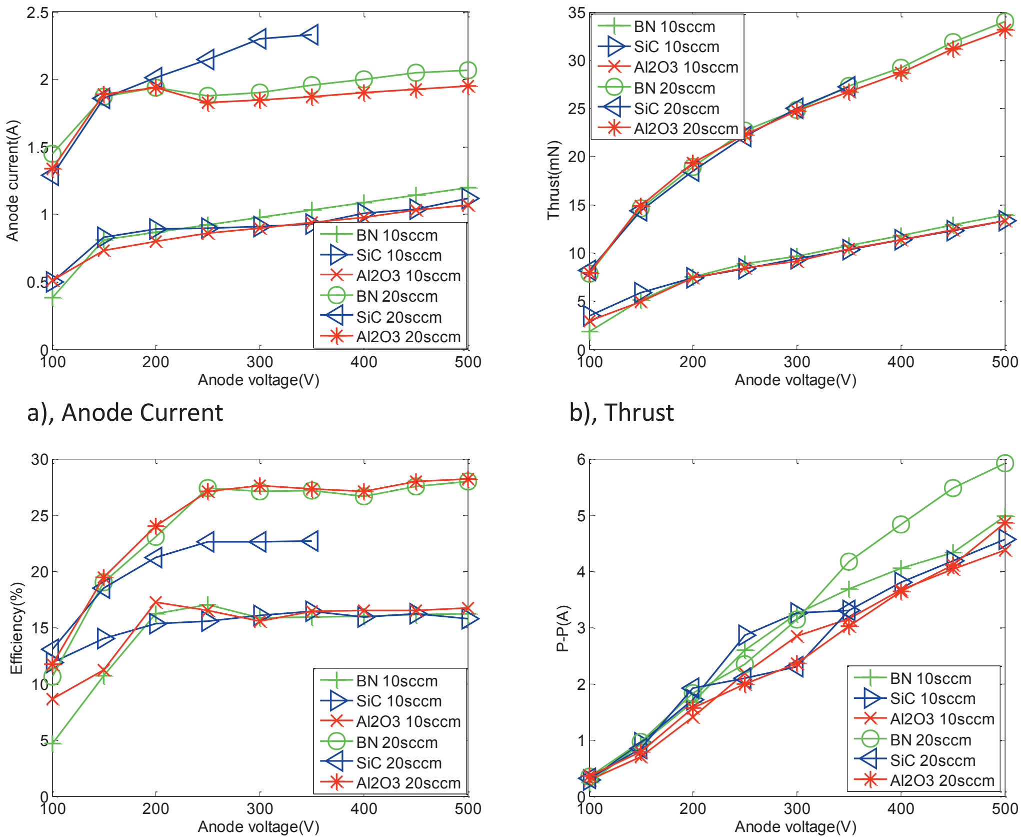

a), Anode Current b), Thrust

c), Anode Efficiency d), Peak-to-Peak Value of Anode Current

Figure 4. Results of performance experiments at constant anode flow rate of 10sccm and 20sccm.

B. Variable-Flow Performance

At a constant anode voltage of 300V, thruster using SiC as channel wall operated on a condition of high current as shown in Fig.5. Especially above 30sccm, the thruster operated unsteadily with the phenomenon of the channel at the cusp reddening. As a whole, the differences of discharge current were obvious and with the relation of SiC > BN > Al_2O_3. The differences of thrust at low anode flow rate were relatively small, but the thrust of BN is obviously bigger than the others wall materials at high anode flow rate. The efficiency of SiC was low because of the biggest electron current. The efficiency differences between BN and Al_2O_3 were relatively small, but the efficiency of BN was bigger than Al_2O_3 above 25sccm. And the peak-to-peak values of anode current oscillation also showed that the thruster operates relatively steadily using Al_2O_3 as wall material.

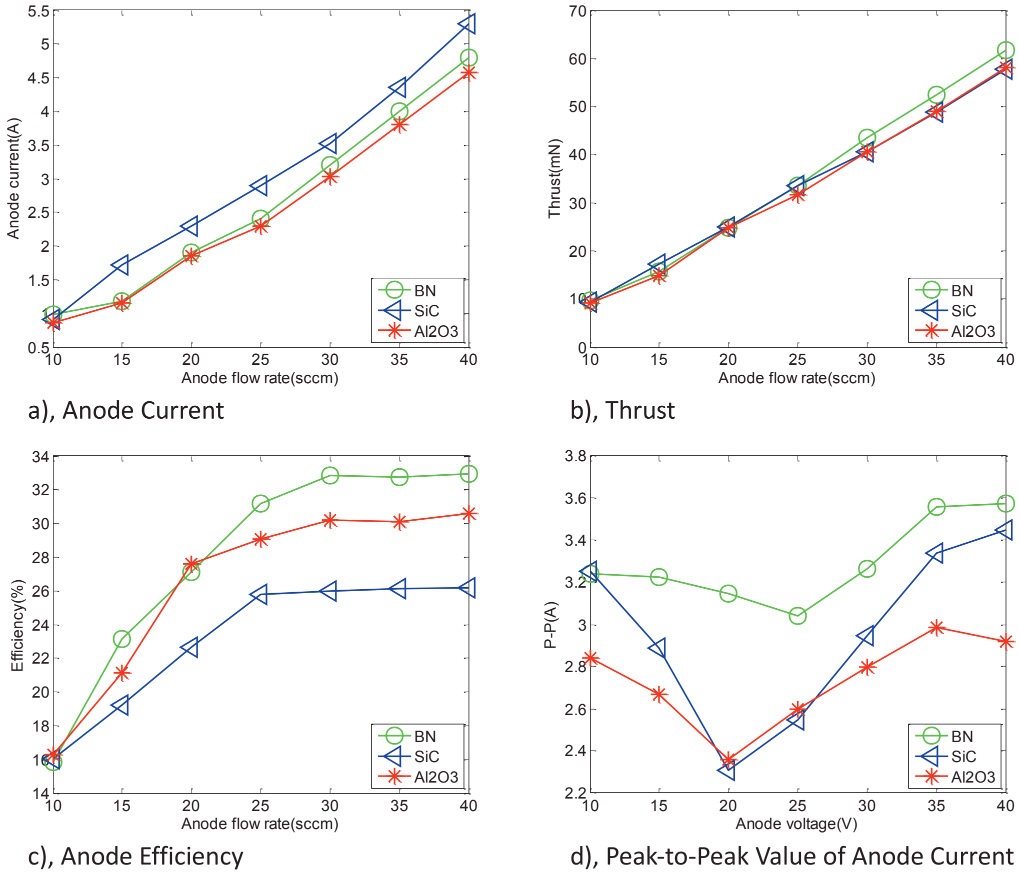

Figure 5. Results of performance experiments at a constant anode voltage of 300V.

IV. Simulation of the Influence of Secondary Emission Yield

Seeing from Fig.4, the efficiency of cusped field thruster using Al_2O_3 as channel wall was higher than using BN as channel wall on some operating conditions of high anode voltage, low anode flow rate. A 2D-3V PIC-MCC model is applied here to study the plasma parameters of such an operating condition, and the simulation models presented in detail in Ref.15. As shown in Fig.6, the length of the simulated channel is 44mm, and the diameter of the channel is 18mm. In the discharge channel, the left lateral boundary is the anode, while the lower and upper boundaries are the symmetric axis and a dielectric wall, respectively. At the same time, a plume region of the thruster is considered in the model. The length of the plume region is 26mm and the diameter is 60mm. Secondary electron emission model is considered at the dielectric walls. The secondary emission yield of SiC and Al_2O_3 are presented in Ref.10, respectively. The neutral velocity V_n = 400m/s and discharge voltage U_d = 300V are applied at the anode, and 0V is applied at the cathode. The results are as following:

A. Potential Distribution and Electron Temperature Profile

Seeing from Fig.6, the electric-field profiles of cusped field thruster have some general characteristics for all wall materials. It can be found that above 200V electric potential drop lies at the last separatrix near channel exit, whereas only about 20V electric potential drop forms near the anode. It means that the main electric potential drop focuses at the last separatrix, which has also been found in recent experiments and simulations. It should also be mentioned that there is still about 40V electric potential drop in the plume region, as has been validated in experiments. As a whole, the effect of secondary emission yield on potential distribution is relatively small.

The statistic electron temperature profiles of thruster with three wall materials are shown in Fig.7. The electron temperature distribution is related to the potential distribution, and electrons are accelerated through electric field, while cooled by the collisions with neutral gas and channel wall. Compared with the potential distribution in Fig.6, the peak of the electron temperature occurs near the cusp 2 region and almost on the centerline, where the most potential drop is located in. In addition, electron temperature on the right of the cusp 2 is relatively lower than the left. It is caused by the gradual energy loss by ionization because of the confine of electrons. For wall materials BN, SiC, Al_2O_3, the peaks of electron temperature are 210eV、200eV、185eV (caused by secondary electron emission), respectively. The averages of electron temperature are 9.26eV、9.16eV、9.61eV, respectively. It is because that the average of electron temperature in computational area is related to the electron temperature and electron number. And the material with high secondary emission yield increases the electron number, while decreases the electron temperature, and thus there is an optimum value of secondary emission yield making average of electron temperature maximum.

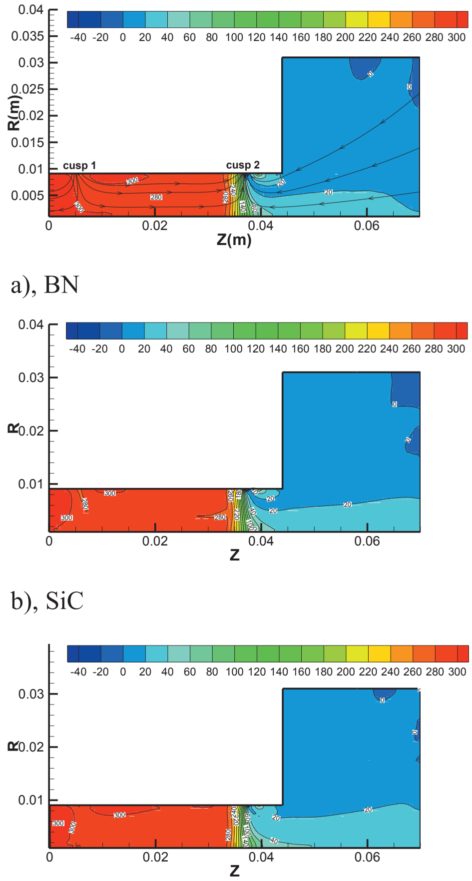

a), BN

b), SiC

c), Al_2O_3

Figure 6. Potential (V) distributions.

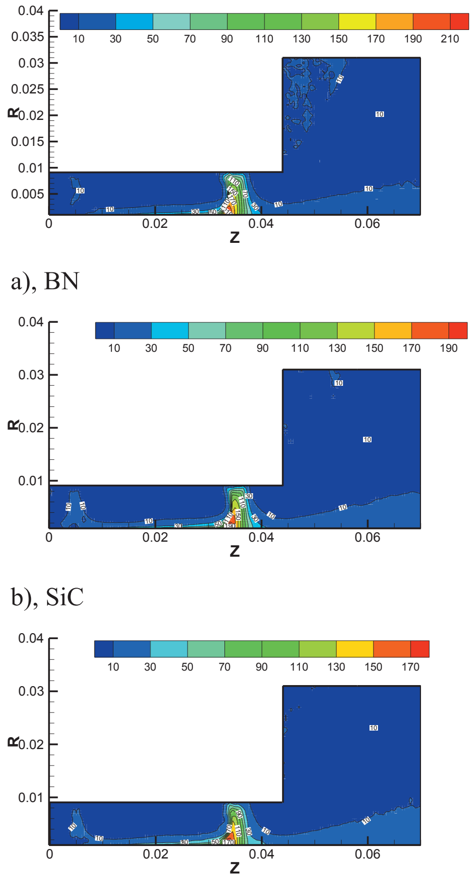

a), BN

b), SiC

c), Al_2O_3

Figure 7. Electron temperature (eV) profiles

B. Electron and Ion Density Profile

The simulation results of the electron and ion density profiles are presented in Fig.8 and Fig.9. For wall materials BN, SiC, Al2O3, the peaks of the electron density occur on the right of the cusp 1 region with the values of 2.9×10^{18}、3.6×10^{18}、3.6×10^{18}, while the ion density reaches its peaks of 2.3×10^{18}、2.6×10^{18}、2.7×10^{18} at the same region. It is because that when electrons arrived at the second separatrix region, most of them have already obtained enough energy to ionize atoms due to the acceleration by the main potential drop near the thruster exit. On the other hand, those electrons following along magnetic field lines will be bounced back due to the magnetic mirror effect, which results in a strong confinement of electrons near the separatrix and an increase of the ionization rate there. And the area with the density exceeding 10^{18} extends with the increase of the secondary emission yield. So on some operating conditions of high anode voltage, low anode flow rate, the efficiency of cusped field thruster using Al_2O_3 as channel wall can be higher than using BN as channel wall.

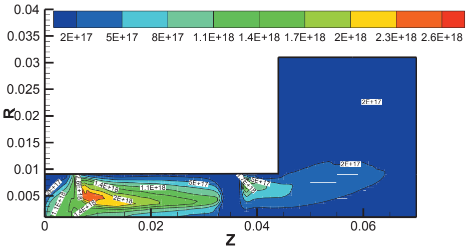

a), BN

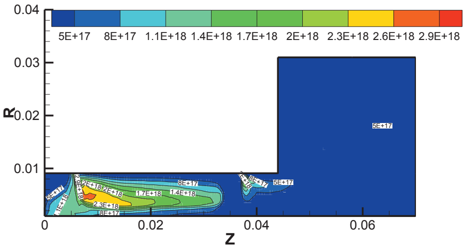

b), SiC

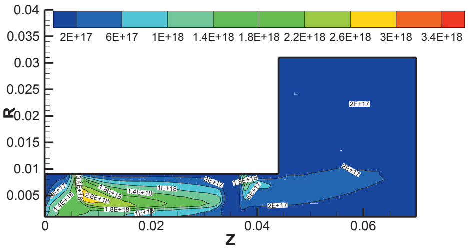

c), Al_2O_3

Figure 8. Electron density profiles.

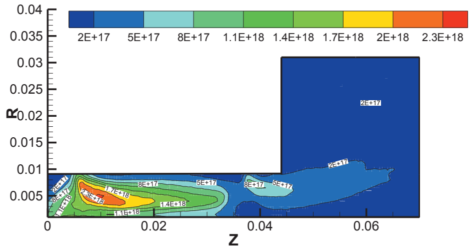

a), BN

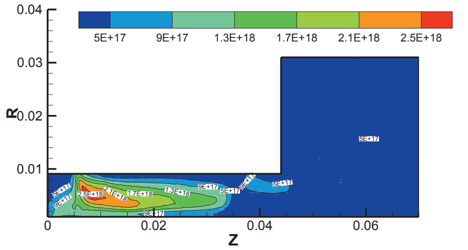

b), SiC

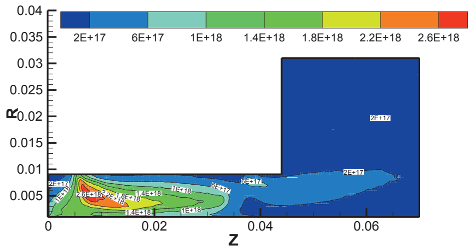

c), Al_2O_3

Figure 9. Ion density profiles.

V. Conclusion

For cusped field thruster using SiC as channel wall, discharge current increasing quickly at a relatively high power can't be explained by Secondary Electron Emission (probably caused by thermally induced failure of the magnetic field), while its performances at low power are comparable to the others wall materials. As a whole, the differences of thrust are relatively small for three materials. On some operating conditions of high anode voltage (above 300V), low anode flow rate, Al_2O_3 with high secondary emission yield has the smallest discharge current, and thus the highest efficiency. That makes it possible to use Al_2O_3 as the channel wall of cusped field thruster on a small-thrust mission. The simulation results of PIC-MCC model also prove that. On some operating conditions of high anode voltage (above 300V), high anode flow rate (25sccm), the efficiency of BN with low secondary emission yield is higher than the others. To achieve the optimal performance, secondary emission yield of material needs match with the operating conditions. And the peak-to-peak values of anode current oscillation shows that the thruster operates relatively steadily using Al_2O_3 as wall material.

References

[1] A. Genovese, A. Lazurenko, N. Koch, S. Weis, M. Schirra, B. van Reijen, J. Haderspeck, P. Holtmann., "Endurance Testing of HEMPT-based Ion Propulsion Modules for SmallGEO," IEPC-2011-141.

[2] Kornfeld, G., Koch, N., & Coustou, G., "First Test Results of the HEMP thruster concept," IEPC-2003-112.

[3] Gildea, S. R., Matlock, T. S., Lozano, P., & Martinez-Sanchez, M., "Low frequency oscillations in the diverging cusped-field thruster," *Proc. 46th AIAA/ASME/SAE/ASEE Joint Propulsion Conf. & Exhibit*, AIAA-2010-7014.

[4] Matlock, T., Gildea, S., Hu, F., Becker, N., Lozano, P., & Martinez-Sanchez, M., "Magnetic field effects on the plume of a diverging cusped-field thruster," *Proc. 46th AIAA/ASME/SAE/ASEE Joint Propulsion Conf. and Exhibit*, AIAA 2010-7104

[5] MacDonald, N. A., Young, C. V., Cappelli, M. A., & Hargus Jr, W. A., "Ion velocity and plasma potential measurements of a cylindrical cusped field thruster," *Journal of Applied Physics*, 111(9), 2012, 093303.

[6] Gascon, N., Dudeck, M., & Barral, S., "Wall material effects in stationary plasma thrusters. I. Parametric studies of an SPT-100," *Physics of Plasmas (1994-present)*, 10(10), 2003, 4123-4136.

[7] Ashkenazy, J., Raitses, Y., & Appelbaum, G., "Parametric studies of the Hall current plasma thruster," *Physics of Plasmas (1994-present)*, 5(5), 1998, 2055-2063.

[8] Meezan N B, Gascon N and Cappelli M A., "Linear Geometry Hall Thruster with Boron Nitride and Diamond Walls," IEPC-2001-039.

[9] Bugrova, A. I., Morozov, A. I., & Kharchevnikov, V. K., "Experimental investigation of near wall conductivity," Sov. J. *Plasma Phys*, 16(12), 1990, 849-856.

[10] Barral, S., Makowski, K., Peradzyński, Z., Gascon, N., & Dudeck, M., "Wall material effects in stationary plasma thrusters. II. Near-wall and in-wall conductivity," *Physics of Plasmas (1994-present)*, 10(10), 2003, 4137-4152.

[11] Schneider, R., Matyash, K., Kalentev, O., Taccogna, F., Koch, N., & Schirra, M., "Particle‐in‐Cell Simulations for Ion Thrusters," *Contributions to Plasma Physics*, 49(9), 2009, 655-661.

[12] Gildea, S. R., & Batishchev, O., "Fully kinetic modeling of a divergent cusped-field thruster," Ph.D. Dissertation, Department of Aeronautics and Astronautics, Massachusetts Institute of Technology, Cambridge, Massachusetts, 2009.

[13] Zhao, Y. J., Liu, H., Yu, D. R., Hu, P., & Wu, H., "Particle-in-cell simulations for the effect of magnetic field strength on a cusped field thruster," *Journal of Physics D: Applied Physics*, 47(4), 2015, 045201.

[14] Liu, H., Sun, G., Zhao, Y., Chen, P., Ma, C., Wu, H., & Yu, D., "Plume Control of a Cusped Field Thruster," *IEEE Transactions on Plasma Science*, 43(1), Jan. 2015, 127-129

[15] Liu, H., Wu, H., Zhao, Y., Yu, D., Ma, C., Wang, D., & Wei, H., "Study of the electric field formation in a multi-cusped magnetic field," *Physics of Plasmas (1994-present)*, 21(9), 2014, 090706.